Modeling of the X-irradiation Response of the Carrier Relaxation Time in P3HT:PCBM Organic-Based Photocells

Kenneth Kambour, Nadav Rosen, Camron Kouhestani, Duc Nguyen, Clay Mayberry, Roderick A. B. Devine, A. Kumar, C.-C. Chen, Gang Li, and Yang Yang

***Abstract*—Initial experimental work has demonstrated that x-ray bombardment of organic-based photocells (specifically P3HT:PCBM-based) leads to a reduction in the open-circuit voltage ($V_{\rm oc}$) without apparent change in the carrier relaxation time. The variation of $V_{\rm oc}$ was suggested to be due to the injection and trapping of holes near the anode, which resulted in a decrease in the built-in potential. We have extended the experimental measurements to higher total dose (~ 1300 krad(SiO_2)). Using standard inorganic modeling tools, a device model of the organic cell has been developed and predictions made. These predictions have been compared to the results of the previous and new experimental measurements and they demonstrate reasonable agreement between the two, thereby supporting the initial charge buildup hypothesis. Questions about the origin and behavior of the photo-carrier relaxation arise.**

***Index Terms*—Simulation, solar cells, x-rays.**

I. Introduction

THE need for inexpensive, dependable, radiation-hard solar cells for use in space applications has led to attention being focused on organic polymer solar cells. Such cells are lightweight, flexible and are potentially useful in conformal coverage applications. While these solar cells are less efficient (presently $\sim 8\%$ [1]) than traditional silicon or III–V-based solar cells, the reduced efficiency is compensated for by their lower weight. This leads to a higher specific power (W/kg) and hence a lower fuel cost for launch. Furthermore, their flexibility is a particularly positive attribute since this renders them less vulnerable to vibration damage during the launch process. It must also be added that since one envisages solution processing deposition of the organic cells on very large area sheets (roll-by-roll technology) one can then also imagine a scenario in which a chosen panel area (i.e., a desired wattage) can be simply tailored from a large roll, thereby speeding up the process of solar panel production. This is particularly interesting for rapid assembly/deployment scenarios. Before this somewhat futuristic approach to low-power solar panel production can become a reality for space applications, a full evaluation/understanding of their behavior in a radiation environment is necessary. We have previously reported [2], [3] the results of preliminary X-irradiation studies of the behavior of poly 3-hexyl thiophene:phenyl C61 butyric acid methyl ester (P3HT:PCBM 1:1 by weight)-based photocells. These results are summerized in Fig. 1. The triangles in Fig. 1 represent the relaxation time extracted for different light levels, which result in different $V_{\rm oc}$ values, while the solid circles, solid squares, and open squares represent the results when the light level is held at a constant value (different for each symbol) and the device is irradiated. For total doses up to 300 krad (SiO_2), we observed a reduction in the open-circuit voltage, $V_{\rm oc}$. We have also observed that the optical photo-carrier relaxation time, τ, remained unchanged [2], [3]. To explain the behavior of $V_{\rm oc}$, the hypothesis was advanced that radiation resulted in charging

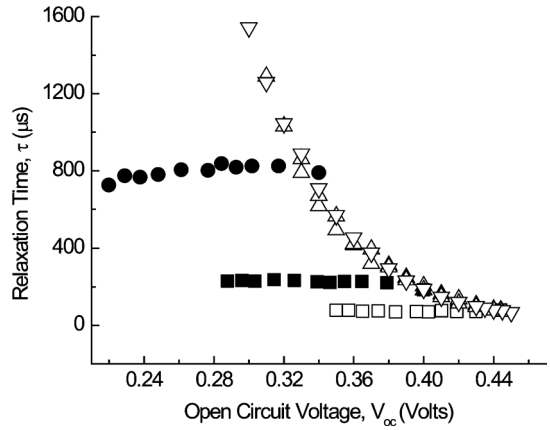

Fig. 1. The experimental relaxation times as a function of the open-circuit voltage. $(\Delta, \nabla)V_{\rm oc}$ is varied by changing the background light level/generation rate. •, ■, □, results when $V_{\rm oc}$ changes due to irradiation, but with different background light levels (resulting in initial $V_{\rm oc}$ values of 0.34 V, 0.40 V, and 0.44 V respectively). A version of the plot with slightly different symbols was reported elsewhere [3].

Manuscript received July 02, 2012; revised September 11, 2012; accepted October 01, 2012. Date of current version December 11, 2012. The work of K. Kambour was supported by the U.S. Air Force under a contract sponsored, monitored, and managed by United States Air Force Air Force Material Command, Air Force Research Laboratory, Space Vehicles Directorate, Kirtland AFB, NM 87117-5776. Work at Kirtland AFB was funded by the AFSOR through AFOSR-09RV01COR. Their work is based on research sponsored by the Air Force Research Laboratory under agreement number FA9453-08-2-0259. The work at UCLA was supported by the Air Force Office of Scientific Research (AFOSR, Grant No. FA9550-09-1-0610, Program manager: Charles Lee Ph.D.).

K. E. Kambour is with SAIC Kirtland AFB, NM 87117 USA (e-mail: kenneth.e.kambour@saic.com).

N. Rosen and C. Mayberry are with the Air Force Research Laboratory, Space Vehicles Directorate Kirtland AFB, NM 87117 USA.

C. Kouhestani and D. Nguyen are with COSMIAC Kirtland AFB, NM 87117 USA.

R. A. B. Devine is with Think Strategically, Kirtland AFB, NM 87117 USA.

A. Kumar, C.-C. Chen, G. Li, and Y. Yang are with Materials Science and Engineering, University of California at Los Angeles, Los Angeles, CA 90024 USA.

Digital Object Identifier 10.1109/TNS.2012.2222666

0018-9499/$31.00 © 2012 IEEE

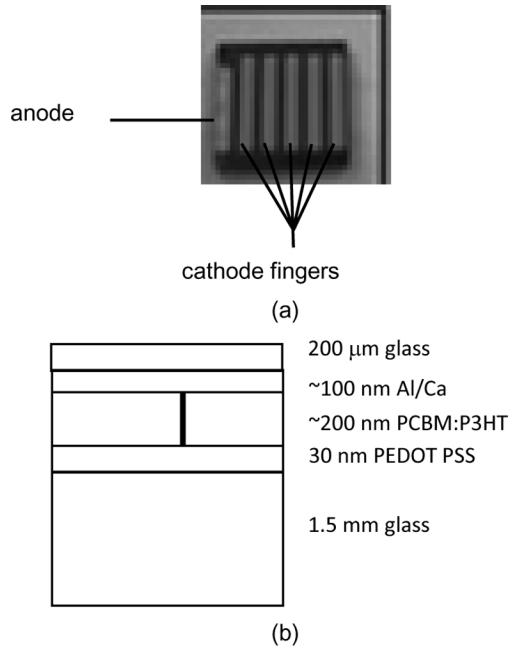

Fig. 2. (a) A picture of one of solar cells (1.5 × 1.5 cm) studied. (b) A schematic drawing of the cross section below a cathode finger of solar cells studied. The single thick line represents the active region simulated by the modeling.

at the photocell contacts and that this charge acted rather like fixed oxide trapped charge in metal-oxide-semiconductor field effects transistors (MOSFETs) by varying $V_{\rm oc}$ in an analagous way to the threshold voltage shifts. Implicit to understanding the experimental x-ray data for the photo-induced carrier relaxation, τ, was the assumption that the trapped charge did not appear to influence it. This assumption, however, is inconsistent with the usual model invoked for photo carrier recombination in which the Langevin mechanism is responsible [4], leading to a $\tau \propto \exp(-{\rm qV_{oc}/kT})$ dependence, i.e., τ varies with $V_{\rm oc}$. In an effort to address these issues and develop a more physical foundation, we have extended our experimental data range (primarily to significantly higher total dose). We have then used traditional commercial device modeling tools and methods usually applied to the study of inorganic devices in order to explore the device behavior from a theory standpoint.

II. Experiment

The experimental set-up has been described elsewhere [2], [3] and is briefly recalled as follows. The P3HT:PCBM 1:1 by weight cells were produced at the University of California, Los Angeles (UCLA) using methods described elsewhere [5], with an example photograph and schematic shown in Fig. 2. They were exposed using an uncalibrated background light source (halogen) that established a mean open-circuit voltage chosen to be within the range 0–0.45 V by varying the light intensity. Superimposed on the chosen background was a pulse of light from a halogen flashtube (also uncalibrated). The duration of the pulse was ~ 2 μs, which was substantially shorter than any of the estimated photo-induced carrier relaxation times we have measured. These pulses, at a repetition frequency of ~ 2 Hz, induced small fluctuations $(\Delta V_{\rm oc})$ of the cell open-circuit voltage

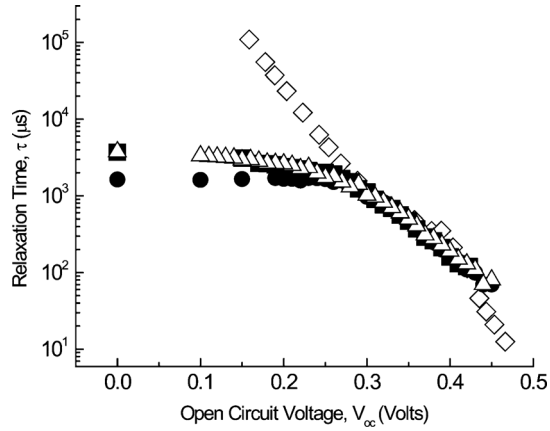

Fig. 3. The experimental (•, ■, Δ) and fitted simulated ($\Diamond$) relaxation times as a function of the open-circuit voltage where $V_{\rm oc}$ is varied by changing the light level/e-h pair generation rate.

as measured using a high input impedance, digitizing oscilloscope. The pulse intensity was usually adjusted during the experiment so that $\Delta V_{\rm oc}/V_{\rm oc}$ was ≤ 0.05—the photo-induced carrier density was then only slightly perturbed by the addition of the pulse. The relaxation of the induced $\Delta V_{\rm oc}$ was assumed to follow an exponential time decay consistent with other authors (see [2], [3] and references therein) with the approximation that $\Delta V_{\rm oc} \propto \Delta n$, where n is the photo-induced carrier density. Relaxation times and open-circuit voltages were determined for different background light levels and following total doses of x-ray irradiation. All measurements were performed *in-situ* in an ARACOR® 4100 irradiation system (Advanced Research & Applications Corp.) using a tungsten target at 45 kV and a current level of 20 mA, yielding a dose rate at the photocell of 427 rad$({\rm SiO_2}){\rm s}^{-1}$, i.e., after taking account of the atenuation in the cover glass. To ensure that there were no effects of dose rate, a series of measurements of $V_{\rm oc}$ (total dose) were carried out for a variety of dose rates as low as 8 rad$({\rm SiO_2}){\rm s}^{-1}$. No observable difference was detected.

III. New Experimental Results

The unirradiated recombination time data shown by the ∇ and Δ symbols in Fig. 1 were obtained for $V_{\rm oc} \geq 0.30$ V whilst the irradiations lead to $V_{\rm oc}$ values as low as ~ 0.23 V, although starting higher. Since the objective of the present study was to irradiate to higher total doses than used to generate Fig. 1, we began by extending the measurements of $\tau(V_{\rm oc})$ for the unirradiated case. The results of measurements on three different devices are shown by the •, ■, and Δ symbols in Fig. 3. Note that τ is shown on a log scale in Fig. 3 and that clearly $\log(\tau)$ is not a linear function of $V_{\rm oc}$. Where the Langevin recombination mechanism ($\tau \propto \exp(-{\rm qV_{oc}/kT})$) [4] is operative, one would have expected to observe a linear relationship of slope q/kT.

The irradiation data shown in Fig. 1 was extended to a total dose of 1300 krad $({\rm SiO_2})$ and the results shown in Fig. 4. We have used 0.3 V, 0.35 V and 0.4 V to be the starting $V_{\rm oc}$. We observe that whereas for lower total dose (~ 300 krad$({\rm SiO_2})$), τ appeared to be independent of $V_{\rm oc}$. At higher doses/lower $V_{\rm oc}$ there is a clear upswing, which occurs dependent upon the initial values of $V_{\rm oc}$ (i.e., for dose $D = 0$ krad$({\rm SiO_2})$). An alternative

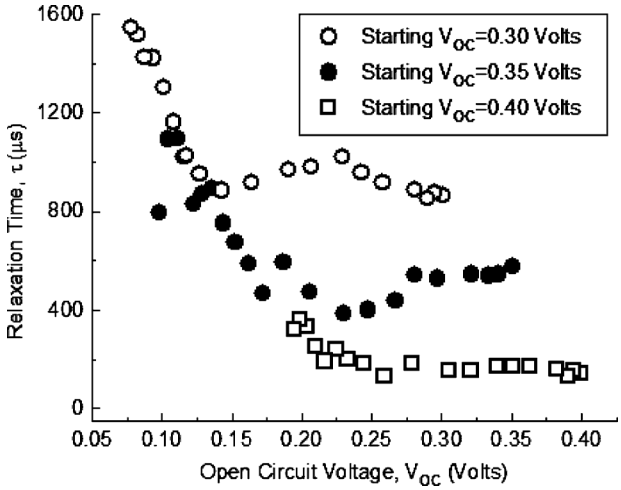

Fig. 4. The experimental relaxation time as a function of the open-circuit voltage for three different pre-irradiation open circuit voltages/light levels.

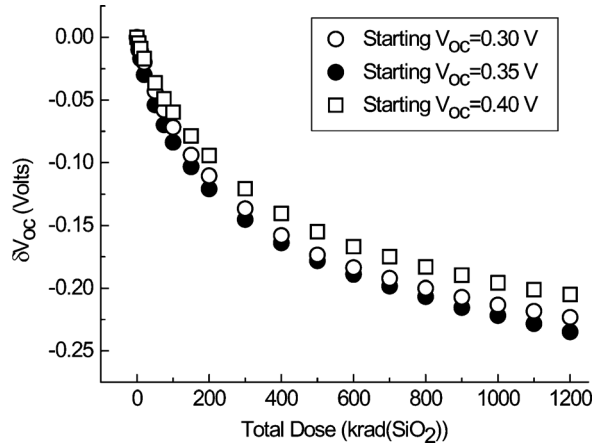

Fig. 6. The experimental variation in the open-circuit voltage as a function of the total dose for three different background light levels/initial $V_{\rm oc}$ values.

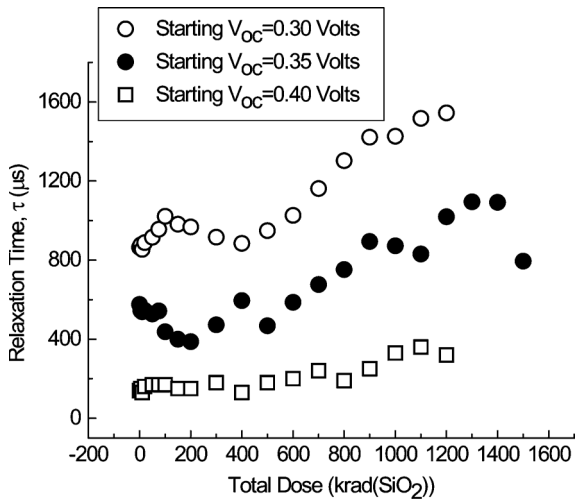

Fig. 5. The experimental lifetime as a function of total dose for three different background light levels/initial $V_{\rm oc}$ values.

representation is shown in Fig. 5 where the measured τ is plotted as a function of total x-ray dose.

Interestingly, whereas previously (Fig. 1) it appeared, to first order, that τ was independent of radiation dose, it is now clear that the recombination time **increases** as the total x-ray dose increases for doses $\geq$400 krad(SiO_2). In Fig. 6 we show the variation in $V_{\rm oc}$ for cells irradiated with different initial $V_{\rm oc}$ values (set by the background, continuous light level) $-\delta V_{\rm oc}$ is the radiation-induced variation of $V_{\rm oc}$. To first order, it would appear that the magnitude of the open-circuit voltage shift is independent of the initial, unirradiated $V_{\rm oc}$ value.

IV. Simulation

Simulations were carried out using SILVACO, Inc.'s ATLAS™ [6]. ATLAS is a physically based commercial device simulator which solves the drift diffusion equations for electrons and holes in the device to predict the electrical behavior of the semiconductor structure, including some models for organic materials [6]. The organic photocells were modeled as a quasi-1D 200 nm thick (this is the approximate thickness of the blend in the experimental devices) material representing the P3HT:PCBM blend, with the anode and cathode contacts attached to the top and bottom, which can be pictured as a line flowing from the cathode shown in Fig. 2(b) to the PEDOT which is treated as the anode. (A number of 2D simulations were done including multiple cathode fingers and no effect on the behavior was noted. Given that the thickness of the device is 200 nm and the effective widths and lengths are in mm or cm, this is not surprising.) The blend was treated as a single material similar to silicon but with a band gap of 1.3 eV, a relative permittivity of 3.4, and conduction and valence band density of states of 2.5×10^{19} cm^{-3}, all of which are commonly accepted for the P3HT:PCBM blend [4], [10]. Initially the carrier mobilities used were also those quoted elsewhere [4], [10] for the blend, but they were eventually lowered in order to obtain a higher quality fit as noted below. The effective built-in potential, $V_{\rm bi}$, was generated by the difference in the work functions between the two contacts [7] and a zero current boundary condition used to calculate $V_{\rm oc}$. In the real device, excitons are injected that either recombine or move to the depletion region and dissociate. In our simulation, this complexity is not included and each light level is assumed to inject a spatially uniform density of electron-hole pairs per second, G.

Of interest from the simulations were the open-circuit voltage and the carrier relaxation time. In order to determine the latter, we simulated the experimental situation. That is to say, we followed experimental methods [2], [8], [9] and "exposed" the device to a spatially uniform electron-hole (e-h) pair generation rate, G, which was allowed to equilibrate. This emulated the effect of the background light source and established an operational $V_{\rm oc}$. Then a short duration ($\sim 2\,\mu$s) additional pulse of e-h pairs was injected causing the $V_{\rm oc}$ to rise by an amount $\Delta V_{\rm oc}$ during the pulse and then decay back to the initial level. As in the experimental measurements, the fitting assumed an exponential variation of $\Delta V_{\rm oc}$ with time, and a relaxation time was extracted. For any situation then, we could determine $V_{\rm oc}$ and τ.

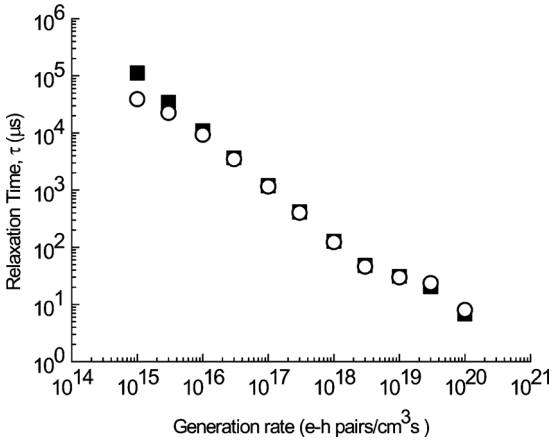

Fig. 7. The simulated relaxation times as a function of the electron-hole generation rate for an anode work function of 4.8eV (○) and 5.0 eV (■).

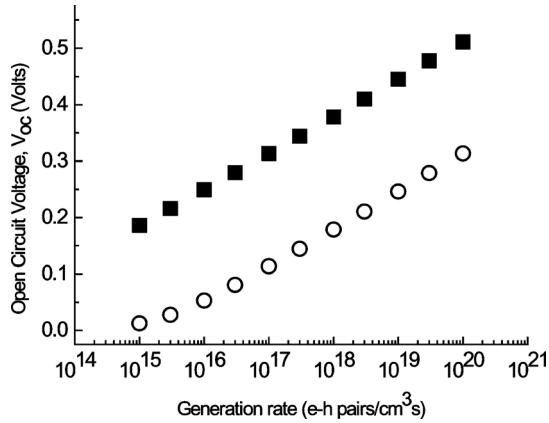

Fig. 8. The simulated open-circuit voltage as a function of the electron-hole generation rate for an anode work function of 4.8eV (○) and 5.0 eV (■).

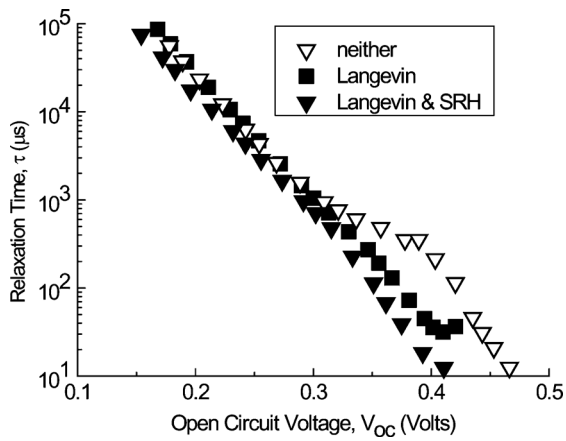

Fig. 9. The effect of recombination mechanism inclusion on the lifetime as a function of open circuit voltage.

V. Simulation Results

A. Unirradiated Devices

The first issue was to determine the open-circuit voltage and the photo-induced carrier relaxation time. Since the relationship between incident light intensity and the e-h pair density generated is not *a priori* known, the generation rate, G, was treated as the independent variable. A wide range of G values was chosen because $V_{\rm oc}$ was expected to depend on the $\log(G)$ [4], [10] and a wide range of $V_{\rm oc}$ was desired to allow comparison with the experimental data. For practical real world uses the effective G would be even higher since the one Sun $V_{\rm oc}$ value for these devices is approximately 0.6 V. The simulation was then performed to determine τ as a function of G (Fig. 7). τ was chosen as the fit parameter since there are only two adjustable parameters in the modeling at this point, the anode material work function and G, and, to first order, the former was found to have little effect on τ, as shown in Fig. 7. Having determined $G(\tau)$, it could then be used in the simulator and $V_{\rm oc}$ fitted to experiment by adjusting the anode work function. As shown in Fig. 8, $V_{\rm oc}$ turned out to be relatively sensitive to the work function so that a precise determination of $V_{\rm oc}$ and τ was possible. In order to achieve a higher quality quantitative match between theory and experiment, it was necessary to set the electron and hole mobilities to 1×10^{-4} and 1×10^{-5} cm/Vs, respectively. This is a factor of 20 less than the values proposed elsewhere [4], [10].

The predicted behavior of $\tau(V_{\rm oc})$ is shown by the ♢ symbols in Fig. 3, where one sees acceptable agreement between theory and experiment at least for $V_{\rm oc}$ values between 0.25 and 0.45 volts, the primary region of interest. Within these limits in both cases $\ln(\tau) = \ln(\tau_o)$-$\beta\ {\rm qV_{oc}/kT}$, where theoretically $\beta = 1$ but is often significantly less than one ($\sim$0.88 for the simulations). For lower $V_{\rm oc}$ values, the experimental results (Fig. 3) show a saturation effect that is not presently predicted in the simulations. The possible reasons for the disagreement between theory and experiment for $V_{\rm oc} \leq 0.25$ V will be discussed later.

As noted above, the matching is reasonable in the region of primary interest. The relaxation time resulting from the simulation described was, in essence, dictated by the time required for the photo-generated carriers to drift to the anode/cathode. In the first instance, therefore, these calculations ignored other recombination processes such as Langevin [6], [10] and Shockley-Reed-Hall (SRH) [6], [11]. The addition of Langevin and Shockley Reed Hall (SRH) recombination to the simulations had a limited effect on the $\tau(V_{\rm oc})$, as can been seen in Fig. 9. Both Langevin and SRH recombination decreased τ at higher $V_{\rm oc}$ values. SRH also slightly decreased the slope $({\rm d}\tau/{\rm dV_{oc}})$ for $V_{\rm oc} < 0.25$ V, even when the SRH lifetimes were as short as 1 ns. Additionally SRH recombination changed the generation rate necessary to achieve a background $V_{\rm oc}$ similar to previous experimental work [10]. In the end, the decision was made to exclude both Langevin and SRH recombination mechanisms from the remaining calculations.

As mentioned previously, a new mystery in this work is the disagreement between the experimental and theoretical values of $\tau(V_{\rm oc})$ for $V_{\rm oc} < 0.25$ V. This saturation effect at very low light levels has been noted experimentally in related quantities in similar cells [12], [13], and its origin is still under investigation. In an analysis of the saturation effect, the first question one might ask is how the magnitude of the pulse-induced $\Delta V_{\rm oc}$ would impact the measurement if $\Delta V_{\rm oc}$ and $V_{\rm oc}$ become of similar magnitude. To examine this, we investigated the effect of the intensity of the 2 μs pulse, i.e., the influence of $\Delta V_{\rm oc}$ via simulation.

According to the simulations, there is a dependence of τ on the change, $\Delta V_{\rm oc}$, produced by the additional light pulse size

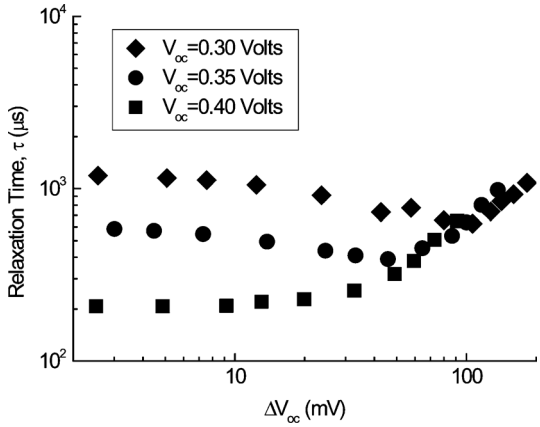

Fig. 10. The simulated relaxation times as a function of change in the open-circuit voltage created by the additional electron-hole/light pulse for three different background open circuit voltages.

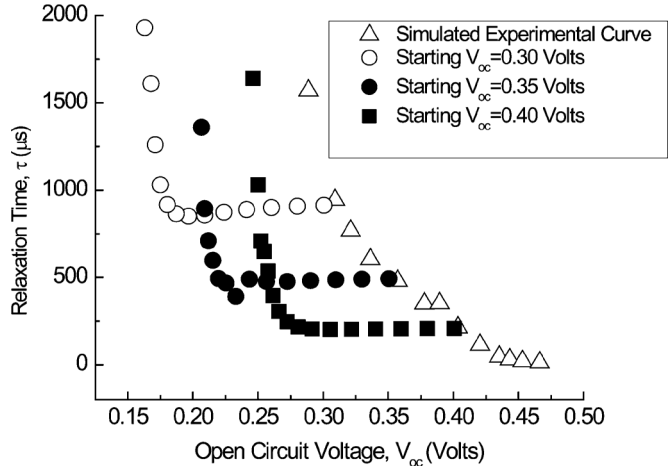

Fig. 11. The simulated relaxation times as a function of the open-circuit voltage. Triangles (Δ) are the results where $V_{\rm oc}$ is varied by changing the light level/generation rate. ■, □, ◯ and • are the results when $V_{\rm oc}$ is changed by adding trapped holes near the anode.

for constant $V_{\rm oc}$. However, based on several trial calculations, shown in Fig. 10, $\Delta V_{\rm oc}$ only appears to modify the predicted τ when it becomes greater than ~ 30 mV, which is substantially larger than in our experiments. Therefore, this does not seem to be the source of the discrepancy between experiment and theory, but it does underscore the need to be working in the small signal regime when working with the low $V_{\rm oc}$ regime.

The most likely explanation, therefore, for the theoretical/experimental disagreement for the behavior of τ for $V_{\rm oc} \leq 0.25$ V is that there is a supplementary unidentified recombination process present which is not included in the simulations at this time. More theoretical work is required in the range $0 \leq V_{\rm oc} \leq 0.25$ V to try to identify this source of recombination.

The mismatch at low $V_{\rm oc}$ does not seem to be a major concern at this time for a number of reasons. First, the goal of this modeling is to explain experimental results most of which are in the range in which good matching is achieved. Secondly, the experimental $V_{\rm oc}$ value at one Sun for these devices is approximately 0.6 V, so the region of mismatch would be at extremely low light levels. As shown in Fig. 8, $V_{\rm oc}$ depends linearly on the $\log(G)$ before saturating at high G values, so small changes in $V_{\rm oc}$ correspond to big changes in G. To put this in perspective, the generation rate needed to match the experimental $V_{\rm oc}$ at 1 Sun is on the order of 10^{23} e-h pairs cm^{-1}s^{-1}, whilst the mismatch between simulation and experiment occurs at $V_{\rm oc} < 0.25$ V corresponding to $G < 3 \times 10^{16}$ e-h pairs cm^{-1}s^{-1}. Thus for most purposes the missing mechanism at low fields is not significant.

B. Irradiation Results

As indicated in Fig. 1, the initial experimental data showed an unusual effect when the device was irradiated with x-rays [2], [3]. The open-circuit voltage decreased (corresponding to the effect of irradiation) without apparent variation of the relaxation time—we argued this decrease in $V_{\rm oc}$ to be due to charge trapping. To test the influence of hole charge trapping on the modeling, the following simulation procedure was adopted. An initial $V_{\rm oc}$ was established by defining an electron-hole pair generation rate together with an anode work function corresponding to an experimental situation (see Fig. 4 for example). Then, maintaining these values, a uniform trapped hole density was placed just inside the anode contact (1 nm from the contact). This charge density was treated as a variable and a plot of τ versus $V_{\rm oc}$ created. The results of such calculations are shown in Fig. 11. The triangles are obtained by varying the background photo-induced e-h generation rates and correspond to the open triangles in Fig. 3, i.e., the unirradiated sample behavior. Note, that here, they are plotted on a linear scale. The other data sets in Fig. 11 (■, □, ◯ and •) represent the effect of trapped holes on devices with different background photo-induced e-h generation rates leading to different initial $V_{\rm oc}$ values. In all cases, $V_{\rm oc}$ is calculated to decrease without any sizeable effects on the relaxation time until an upswing occurs at lower $V_{\rm oc}$ levels (corresponding to higher trapped charge)—these $V_{\rm oc}$ values were lower than those originally studied (Fig. 1) due to lower total x-ray exposures. Initially it was unclear if such an upswing in τ existed, because the major predicted upswings were occurring for $V_{\rm oc} \leq 0.25$ volts—a region in which the unirradiated predictions over predict the lifetimes as shown in Fig. 3. The results of subsequent experiments indicate that the upswing in the relaxation time was confirmed at very high total x-ray doses. This is shown in Fig. 4 and discussed in Section III.

Finally, we should underline that the real variable emerging from this study is the x-ray dose-dependent trapped charge density. When we combine the experimental $\delta V_{\rm oc}$ (total dose) in Fig. 6 with the theoretical variation of $V_{\rm oc}$ with trapped charge density in Fig. 12, we can derive the relationship between the simulated trapped charge density and experimental total x-ray dose. This can be done by assuming that initial $V_{\rm oc}$ value is irrelevant and fitting the data in Fig. 6 to a single function to get $\delta V_{\rm oc}(\rm dose)$ and then fitting Fig. 12 the same way to get $\rho(\delta V_{\rm oc})$. It was found that good fitting can be achieved for $\delta V_{\rm oc}(\rm dose) = A(1\text{-}e^{-\rm dose/B})$, a first order trapping equation. In fitting the dependence of the simulated trapped hole density, $\rho(\delta V_{\rm oc})$, a simple form fits only low carrier densities so $\rho(\delta V_{\rm oc}) = {\rm De}^{\delta {\rm Voc}/E} + F$ is used. (It is worth noting that for $\delta V_{\rm oc} < 0.15$, $\rho(\delta V_{\rm oc})$ is approximately linear, as a simple analysis would suggest, and it is after this region where the sudden upswing in the simulation results occurs.) The fitting allows the calculation of trapped charge density as a function of dose and the result is shown in Fig. 13. Interestingly, we

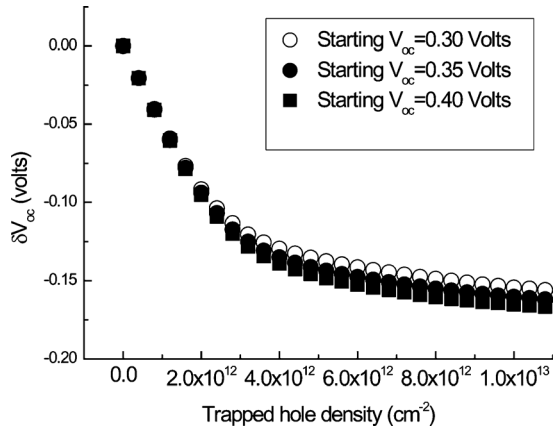

Fig. 12. The simulated change in the open-circuit voltage as a function of the trapped hole density for several different background e-h generation rates/initial $V_{\rm oc}$ values used to generate the $V_{\rm oc}$ changes in Fig. 10.

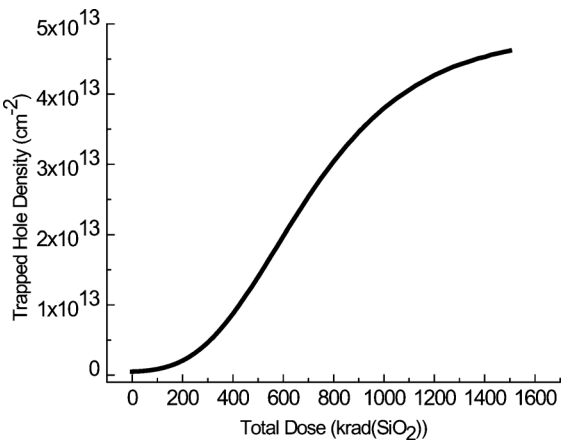

Fig. 13. The fitting based dependence of the trapped hole density on the total x-ray dose.

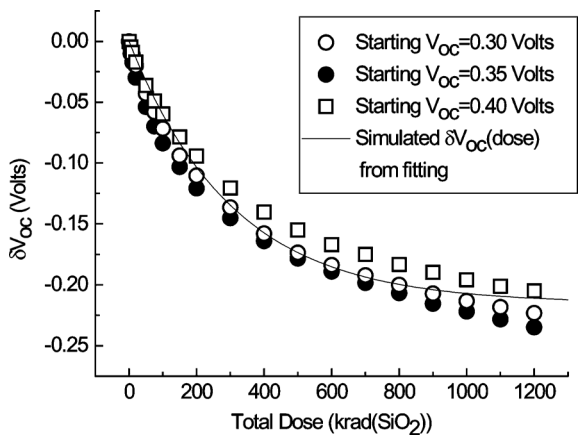

Fig. 14. The experimental change in the open-circuit voltage as a function of the total dose for three different background light levels/initial $V_{\rm oc}$ values plotted with the corresponding values from the simulation fitting.

observe that initially the trapped hole density varies rather slowly $(\text{dose} < 400\ \text{krad}(\text{SiO}_2))$ and then increases. The former corresponds to the regime where τ is essentially constant (Figs. 5 and 11). To test for consistency the $\delta V_{\rm oc}(\text{dose})$ from experiment was compared to the simulated $\delta V_{\rm oc}(\text{dose})$ based on the function shown in Fig. 13 with the results shown in Fig. 14 demonstrating good matching.

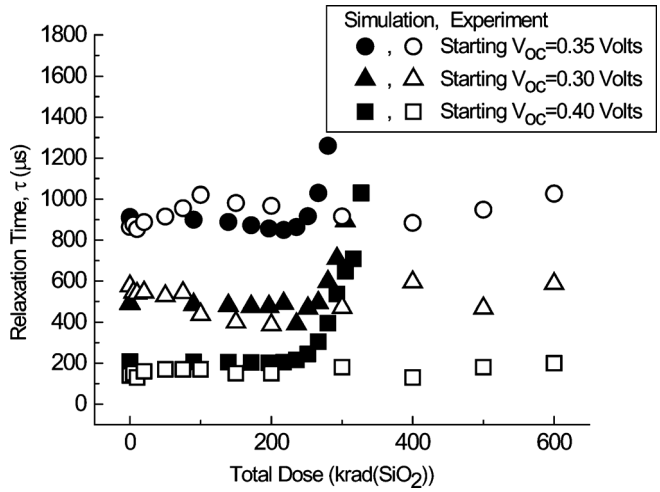

Fig. 15. The experimental (hollow symbols) and simulated (solid symbols) lifetime as a function of total dose for three different background e-h generations rates/initial $V_{\rm oc}$ values.

One can now compare the experimental lifetime (Fig. 5) as a function of dose with the simulated lifetime as a function of dose (Fig. 15). There is qualitative matching although the simulated τ values are numerically larger than experiment. Simulation predicts a $\tau(\text{dose})$ approximately constant for total doses $\leq$ 400 krad(SiO_2) but $\Delta\tau/\Delta$ dose smaller experimentally than predicted thereafter. For example, the experimental lifetime, when the initial $V_{\rm oc} = 0.4$ V, grows by 50% at a dose of 900 krad (SiO_2), but the simulation shows a similar growth at a dose of 300 krad (SiO_2). The reason for this seeming mismatch between simulation and experiment is unclear at this time, though it may be due to the approximate nature of the modeling.

VI. Conclusions

We have extended earlier x-ray exposure measurements on organic semiconductor (P3HT:PCBM)-based photocells to total doses of 1300 krad (SiO_2). Using commercially available device modeling software designed primarily for inorganic semiconductors we have confirmed our earlier hypothesis that radiation-induced open circuit voltage reduction can be interpreted in terms of the build-up of a positively charged layer in close proximity to the anode contact. Experimentally, we have observed that the photo-induced carrier recombination time remains essentially independent of x-ray dose (and hence initial charge build-up) for total doses $\leq$ 400 krad(SiO_2). In our modeling this corresponds to a trapped charge density $\sim 4 \times 10^{12}$ cm^{-2}. Above this charge level, the photo-induced carrier recombination time **increases**.

The dominant mechanisms controlling the recombination time in an unirradiated device is the drift-diffusion time to the contact electrodes. Inclusion of Langevin recombination or Shockley-Reed-Hall mechanisms does not enable us to account for the behavior we have observed experimentally. Therefore, we suggest that as the radiation-induced charge builds up at the anode, it generates a Coulomb repulsion which slows the drift of the photo-generated holes to the anode thereby increasing the effective carrier lifetime.

Why charge does not build up during the light pulse remains unresolved. The most likely reasons seem to be that either the

hole traps are energetically deep and require high energy holes to become charged or that the X-rays generate large numbers of holes allowing a low probability process to happen. Additionally the current simulations do not preclude the idea that the charge is spread throughout the sample as such a volume charge would have an equivalent area contact charge or that electrons could become trapped near the cathode. The sensitivity of the modeling to variability in the input parameters needs to be explored in the future,

We have applied a standard inorganic-based photocell simulator to model organic-based cells. Surprisingly, though this may be an approximation, the qualitative experimental features in radiation-induced build-up of trapped charge and dose-dependent increase of the photo-induced carrier relaxation time are accounted for. Further refinement and expansion of the model is clearly necessary to build on these initial results.

REFERENCES

[1] Y. Liang, Z. Xu, J. Xia, S. Tsai, Y. Wu, G. Li, C. Ray, and L. Yu, "For the bright future-bulk heterojunction polymer solar cells with power conversion efficiency of 7.4%," *Adv. Mater.*, vol. 22, no. E135, 2010.

[2] A. Kumar, R. Devine, C. Mayberry, B. Lei, G. Li, and Y. Yang, "Origin of radiation-induced degradation in polymer solar cells," *Adv. Funct. Mater.*, vol. 20, no. 2729, 2010.

[3] R. Devine, C. Mayberry, A. Kumar, and Y. Yang, "Origin of radiation induced damage in organic HT:PCBM based photocells," *IEEE Trans. Nucl. Sci.*, vol. 57, no. 6, pp. 3109–3109, Nov. 2010.

[4] L. Koster, V. Mihailetchi, R. Ramaker, and P. Blom, "Light intensity dependence of open-circuit voltage of polymer:fullerene solar cells," *Appl. Phys. Lett.*, vol. 86, no. 123509-1, 2005.

[5] G. Li, V. Shrotriya, J. Huang, Y. Yao, T. Moriarty, K. Emery, and Y. Yang, "High-efficiency solution processable polymer photovoltaic cells by self-organization of polymer blends," *Nature Materials*, vol. 4, no. 864, 2005.

[6] *ATLAS User's Manual, Device Simulation Software*. Santa Clara, CA: SILVACO International, 2007.

[7] I. Hwang and N. C. Greenham, "Modeling photocurrent transients in organic solar cells," *Nanotechnology*, vol. 19, no. 424012, 2008.

[8] J. E. Mahan, T. W. Ekstedt, R. Frank, I, and R. Kaplow, "Measurement of minority carrier lifetime in solar cells from photo-induced open-circuit voltage decay," *IEEE Trans. Electron. Dev.*, vol. ED-26, no. 5, pp. 733–739, May 1979.

[9] C. G. Shuttle, B. O'Regan, A. M. Ballantyne, J. Nelson, D. D. C. Bradley, J. de Mello, and J. R. Durrant, "Experimental determination of the rate law for charge carrier decay in a polythiophene: Fullerene solar cell," *Appl. Phys. Lett.*, vol. 92, no. 093311, 2008.

[10] M. M. Mandoc, F. B. Kooistra, J. C. Hummelen, B. de Boer, and P. W. M. Blom, "Effect of traps on the performance of bulk heterojunction organic solar cells," *Appl. Phys. Lett.*, vol. 91, no. 263505-1, 2007.

[11] S. M. Sze, *The Physics of Semiconductor Devices*. Wiley, NY: , 1981, ch. 1.

[12] P. P. Boix, J. Ajuria, R. Pacios, and G. Garcia-Belmonte, "Carrier recombination losses in inverted polymer: Fullerene solar cellswith ZnO hole-blocking layer from transient photovoltage and impedance spectroscopy techniques," *J. Appl. Phys.*, vol. 109, no. 074514, 2011.

[13] P. P. Boix, A. Guerrero, L. F. Marchesi, G. Garcia-Belmonte, and J. Bisquert, "Current-Voltage characteristics of bulk heterojunction organic solar cells: Connection between light and dark curves," *Adv. Energy Mater.*, vol. 1, no. 1073, 2011.